ISSN: 0975-8585

Research Journal of Pharmaceutical, Biological and Chemical Sciences

Synthesis of hydroxyappatite nanoparticles by emulsified liquid membrane technique. Part I: Study of membrane stability.

Rania M Sabry, Azza I Hafez*, and Maaly MA Khedr.

Chemical Engineering and Pilot Plant Dept., National Research Centre, Cairo, Egypt.

ABSTRACT

An extensive experimental study for synthesis of hydroxylappatite (HAp) nanoparticles using emulsion liquid membrane technique (ELM) was undertaken. The studied parameters, expected to have the greatest influence on the stability of the emulsified liquid membrane and consequently on the HAp nanoparticle synthesis, are: emulsification time (5-15 minutes), emulsification rotating speed (8000-14000 rpm), mixing speed (200-450 rpm), type and concentration of carrier (3-9% w/v of D2EHPA and n-caproic acid), type and concentration of surfactant (3-9% w/v of Spans 20, 80 and 83) and the type of organic solvent (kerosene, iso-octane, heptane, hexane and toluene). The synthesized HAp nanoparticles were characterized by means of XRD, TEM, FTIR, SEM and EDX. Needle-like HAp nanoparticles ranging from 3-7 nm in diameter and 27-46 nm in length were obtained at optimum ELM stability conditions.

Keywords*:* Emulsion liquid membrane, hydroxyapatite, nanoparticles, surfactants, carrier, and solvent.

Corresponding author

ISSN: 0975-8585

INTRODUCTION

The synthesized calcium phosphate compounds have generated a great deal of interest because of the wide variety of their medical applications, especially in orthopedics, plastic and dental surgeries. Among these compounds, hydroxyapatite, (HAp) [$Ca_{10}(PO_4)_6(OH)_2$] has attracted much attention as a material for biomedical applications. Due to the chemical similarity between HAp and mineralized bone of human tissue, synthetic HAp exhibits strong affinity to host hard tissues. However, due to poor mechanical properties of micro-size HAp, the recent trend in bio-ceramic research is focused on improving their mechanical and biological properties using nanotechnology. Multiple techniques for the preparation of hydroxyapatite nanoparticles have been developed over the past decades including hydrothermal methods [1**]**, sol-gel methods [2] mechano-chemical methods [3] chemical precipitation methods [4] and recently liquid membrane methods [5-8]. Liquid membrane (LM) is a liquid phase, usually organic, interposed between two miscible aqueous solutions. Extraction and stripping processes take place concurrently: at one side of the membrane (feed solution) the material to be transported is extracted, while at the other side (stripping solution) re-extraction occur [9]. Several LM configurations were reported, differing mainly in the membrane performance, among these, the emulsion liquid membrane (ELM) is the objective of the present work. The main advantages of the ELM system are: (a) high interfacial area for mass transfer; (b) high diffusion rate of the metal ion through the membrane and (c) capability of treating variety of element and compounds in industrial setting at greater speed and with a high degree of effectiveness, with varying contaminant concentration and volume requirements. Many successful applications of ELMs for separation processes in general, and especially for removal of heavy metal ions from wastewaters, have been reported in the literature [10-14]. Recently, it has been found that the internal water phase is capable of being used for the preparation of size-controlled and morphology-controlled fine particles, since the micron-sized internal water droplet has a restricted reaction area [15,16]. For such reason, ELM technique is the most promising means for preparation of HAp nanoparticles with narrow size distribution range.

An intensive research program was planned and implemented to investigate one interesting, innovative technique for the preparation of hydroxyapatite in nano form for biomedical applications. The present article is highlighting the importance of emulsion stability to controlling the size and morphology of synthesized nanoparticles.

Emulsion liquid membrane transport phenomena

There are two different configurations for the ELM: (1) oil-in water in- oil (O/W/O) system and (2) water-in-oil-in-water (W/O/W) system. The latter ELM configuration is the target of the present study in which solutes are present in aqueous phase. Generally, ELMs- also called surfactant liquid membranes- are double emulsions composed by emulsifying two immiscible phases, e.g., either water droplets (internal stripping phase or receptor)- stabilized by oil soluble surfactants- dispersed as very fine droplets (1-10µm) in an oil phase (W/O), or vice versa (O/W), and further dispersing the resulting emulsion (liquid membrane) in another aqueous, [external feed (or donor) phase], as emulsion globules (0.1-2mm) containing the target solute to be removed, which is the Ca^{2+} in this study. In this (W/O/W) ELM, the oil phase acts as a selective membrane, as illustrated in Figure (1).

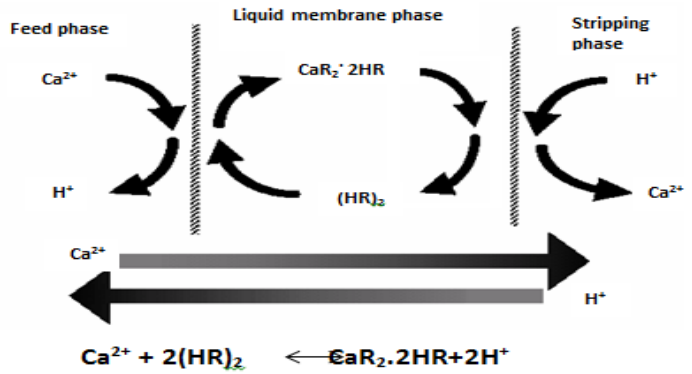

Figure (1) Model for Ca^{2+} permeation through the liquid membrane phase for HAp preparation.

During this process, calcium ions in the feed solution diffuse toward the feed membrane interface, where complex formation between Ca^{2+} and a carrier (HR) occur. Carrier exists as the dimmer $(HR)_2$ in the organic solvent. This carrier should be insoluble in both the feed and the stripping phases, and should react specifically and reversibly with permeate. Thus, the complex ($CaR_2.2HR$) diffuses in the membrane and on reaching the stripping membrane interface, hydrogen ion (H^+) in the stripping solution reacts with the complex to liberate the calcium ion. This step regenerates the carrier $(HR)_2$ which then diffuses back to the feed side of the membrane and the entire process is repeated. The solute mass transfer is driven by the concentration difference between the external feed phase and the internal stripping phase. Thus, calcium ions can be pumped from a lower concentration solution into a higher concentration one through the liquid membrane because its flow is coupled to a flow of hydrogen ions in the opposite direction [17].

MATERIALS AND METHODOLOGY

Materials.

Chemicals used in the experimental study are:

- *Surfactant :* 1-Span 20 (sorbitanmonolaurate), 2-Span 80 (sorbitanmonooleate), 3- Span 83 (sorbitansesquioleate), all from Sigma Chemical Company.
- *Carrier:*1-Bis-(2-ethylhexl)phosphoric acid ($C_{16}H_{35}O_4P$),commercially named [D2EHPA], assay ≥ 95%, Merck, 2- n-caproic acid ($C_6H_{12}O_2$), ≥ 98%, Fluka.
- *Organic solvent:*1- commercial kerosene ,Misr Petroleum Company, 2- Iso-octane [2,2,4-trimethyl pentan])(C_8H_{18}), assay≥95%, Arabian Medical and Scientific Lab., 3-n-heptane($CH_3(CH_2)_5CH_3$), assay ≥ 95% Lab-Scan, Analytical Science, 4-Hexane ($CH_3(CH_2)_4CH_3$), assay ≥ 95%, Fluka, 5-Toluene ($C_6H_5CH_3$), assay ≥ 95%, Fluka.
- *Phosphoric acid:* Analar ,BDH laboratory suppliers.
- *Calcium nitrate tetrahydrate ($Ca(NO_3)_2.4H_2O$):* assay ≥ 99%, Merck.
- *Ammonia solution:* assay 25%, ADWIC.

Methodology.

Experimental Procedure:

ELM breaking rate experiment

Water/oil (W/O) emulsion is prepared by mixing equal volumes of the internal phase, consisting of an aqueous solution of 0.5 mol H_3PO_4 and the organic membrane phase composed by pre-determined components, namely, organic solvent, surfactant and carrier. Firstly, the internal phase is added drop-wise to the stirred organic phase to reach 1:1 volume ratio of organic membrane solution to stripping solution. The two phases are mixed together and emulsified by means of a mechanical homogenizer (Wise Mix™ Digital Homogenizer HG 15D, Korea), at high fixed rpm to certain emulsification time, resulting in a white emulsion. Afterwards, in a 250 ml beaker, a certain volume of the above resulting emulsion is poured into 100 ml of redistilled water as external aqueous phase solution. The as-prepared solution mixture is then vigorously stirred by means of a variable speed motor driven stirrer (VELP Scientifica, Italy) at a fixed speed to disperse W/O emulsion droplets forming the W/O/W emulsion. After a pre-set stirring time, the double emulsion (W/O/W) is left in a separating funnel to allow aging and separating the W/O emulsion from the external aqueous phase. The feed phase is filtered to avoid any entrained emulsion droplets, and the pH of the filtrate is then measured for emulsion membrane breaking rate percent determination.

ELM extraction efficiency experiment:

Since the ELM extraction efficiency depends greatly upon its stability, the ELM performance at each studied parameter was investigated by using 0.5 molar calcium nitrate tetra-hydrate solution, as source of Ca^{2+} ion, instead of re-distilled water, as external aqueous phase where its pH was adjusted to a pre-set point by 25% concentrated ammonium solution. In this case, the residual calcium ions in the external phase (filtrate) is measured by atomic absorption (PerkinElmer analyst 800, USA)as indication of ELM efficiency. The resulting

upper emulsion phase is washed with redistilled water, followed by centrifugation (EBA 20, Hettich, Germany) at 5000 rpm to remove the external aqueous phase residue. The W/O emulsion is then demulsified by adding ethanol followed by centrifugation to separate the solid particles (product) from the organic membrane. The particles obtained are finally dried at 80 °C for 2 hours.

Emulsion stability measurement:

From the practical point of view, the stability of W/O/W emulsions is generally understood as the resistance of the individual globules against coalescence. Hence, as membrane breaking up causes a decrease in the extraction performance, the percent breaking rate model is adopted herein, for stable emulsion measurement, among the different stability determination criteria.

In this model, the pH variation of the external phase (re-distilled water) with time is an indication of the emulsion breaking. The breaking rate (BR) is defined as the fraction percent of the expulsed internal phase volume to external phase [18] as represented in equation (1).

$$BR\% = \frac{Vr}{Vint} x100 \qquad (1)$$

Where V_r and V_{int} are the breaking volume and the initial internal phase respectively.
The volume V_r is calculated by material balance of the external phase measure before and after contact, viz:

$$Vr = Vext\left\{\frac{10^{-pHo} - 10^{-pH}}{10^{-pH} - [H+]i}\right\} \qquad (2)$$

Where: V_{ext} is the initial external phase volume, pH_o is the pH of the initial external phase, pH is the pH of the external phase being in contact with the emulsion after a certain time of agitation and the $[H^+]_i$ is the protons of initial concentration in the internal phase.

Characterization:

- Fourier transform infrared (FTIR) spectroscopy analysis was performed for functional groups identification, using Shimadzu Japan FTIR-8700 spectrophotometer. Measurements were carried out in the mid-infrared range (400-4000 cm^{-1}). The prepared nanoparticles were previously mixed with KBr, homogenized and converted to pellets under a pressure of 8 ton_f .
- The crystallographic structural analysis of the product was determined by X-ray diffractometer (D8-Advance,Bruker, Germany), using Cu Kα radiation (λ=0.15418nm) at the X-ray voltage of 40kV and current tube 40 mA.
- Scanning electron microscopy (SEM) was performed for sample surface topography with JEOL (SEM-840A, Japan) electron microscope, operating at acceleration voltage of 80KV.Particles samples were spread onto a copper wafer and subsequently sputtered with gold (250 Å) before testing.
- Transmission electron microscopy (TEM) was undertaken with JEOL (TEM-1230, Japan) electron microscope, operating at acceleration voltage of 100KV. Samples, dispersed in ethanol were transported to carbon coated copper grids and left to dry before testing,

4. RESULTS AND DISCUSSION

Effect of emulsification time at different emulsification speed.

ELM stability

Figure (2) shows the influence of emulsification time (5-15 minutes) on the emulsion stability in terms of percent breaking rate (BR %) at different emulsification rotating speed (8000 – 14000 rpm), and constant other operating parameters ,i.e., 400 rpm as mixing speed, 4% w/v of D2EHPA as type and carrier concentration, 4% w/v of Span 80 as surfactant and kerosene as organic solvent. It was observed that, the breakage percentage of W/O emulsion decreases gradually with increasing the emulsification rotating speed

at constant time because an efficient emulsification speed gives a good dispersion of internal phase droplets into the membrane. This fact means that when these droplets become smaller, they will take much more time to coalesce, which results in a good stability of W/O emulsion. Moreover, when the emulsification time increases the emulsion stability increases only at emulsification speeds 8000 and 10000 rpm, while at 12000 rpm & 14000 rpm no significant effect is observed on the emulsion stability. Therefrom, 5 minutes emulsification time and 14000 rpm emulsification rotating speed rather than 1200rpm- as it gives better performance- are taken as optimum conditions for ELM stability.

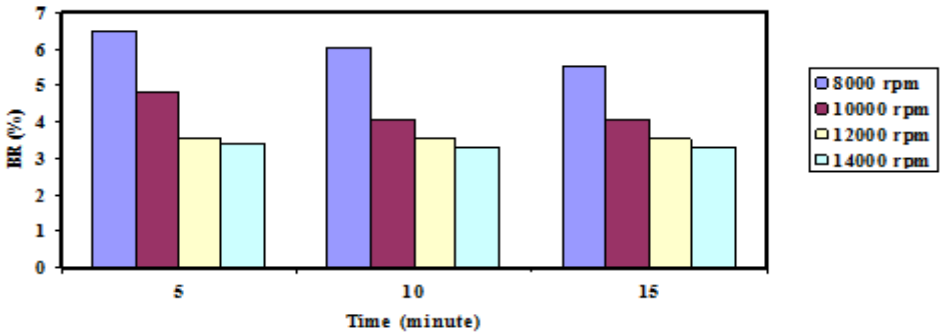

Figure (2):Effect of emulsification time on the emulsion stability at different emulsification rotating speed, 400rpm mixing speed, 4% w/v carrier conc., 4% w/v surfactant conc.& kerosene.

ELM efficiency

At similar experimental conditions as mentioned above, the effect of emulsification time on HAp nanoparticle formation at different emulsification rotating speed was investigated and demonstrated in Figure (3). The extraction efficiency of calcium ions increased gradually from 94.35% to 97.3% with increasing the emulsification rotating speed from 8000 rpm to 14000 rpm.

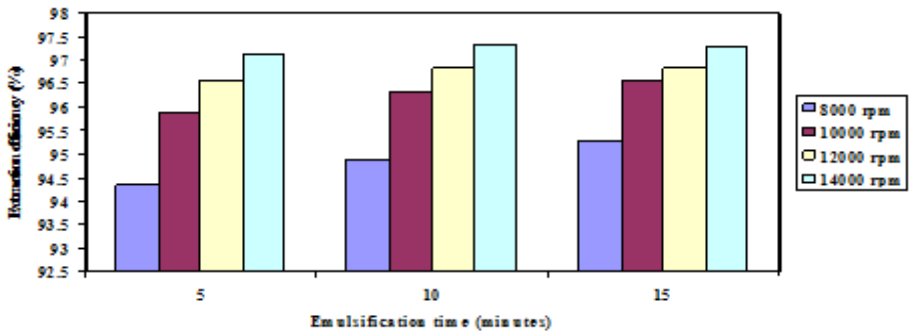

Figure (3) Effect of emulsification time on the extraction efficiency of calcium at different emulsification rotating speed, 400 rpm mixingspeed, 4% w/v carrier conc. and 4% w/v surfactant conc.& kerosene. (5% w/v) and organic solvent (kerosene).

While the effect of emulsification time on the extraction efficiency of calcium ions have the same behavior as mentioned above in the case of emulsion stability.

Characterization:

Figure (4) shows the Fourier FTIR spectra of the prepared HAp nanoparticles at different emulsification speed and time. The first indication of the formation of HAp nanoparticles is the form of broad FTIR band centered at about 1000-1100 cm^{-1}[19]. The vibration band around 874 cm^{-1} have been assigned as signature peaks for brushite [$CaHPO_4(H_2O)_2$] indicating the presence of HPO_4^{2-} group [20]. A broad band between 3400-3500 cm^{-1} has been observed due to the stretching mode of H bonded OH or water conforming the formation of Hap. As observed from Figure (4), the peak intensity and sharpness of the absorption bands at

ISSN: 0975-8585

560-601cm^{-1} and 930-1100 cm^{-1} derived from PO_4^{-3} are influenced by emulsification speed and time: by increasing the emulsification speed with time the peak intensity and sharpness of the absorption bands also increases. It is generally accepted that the peak intensity and sharpness of these absorption bands are indications of the degree of crystallinity. In the present study, the above observation indicates and proves that the crystallinity of the product is affected by the emulsion stability. In a word, the results of FTIR spectra indicates that the prepared product is HAp nanoparticles with additional phase of calcium phosphate family.

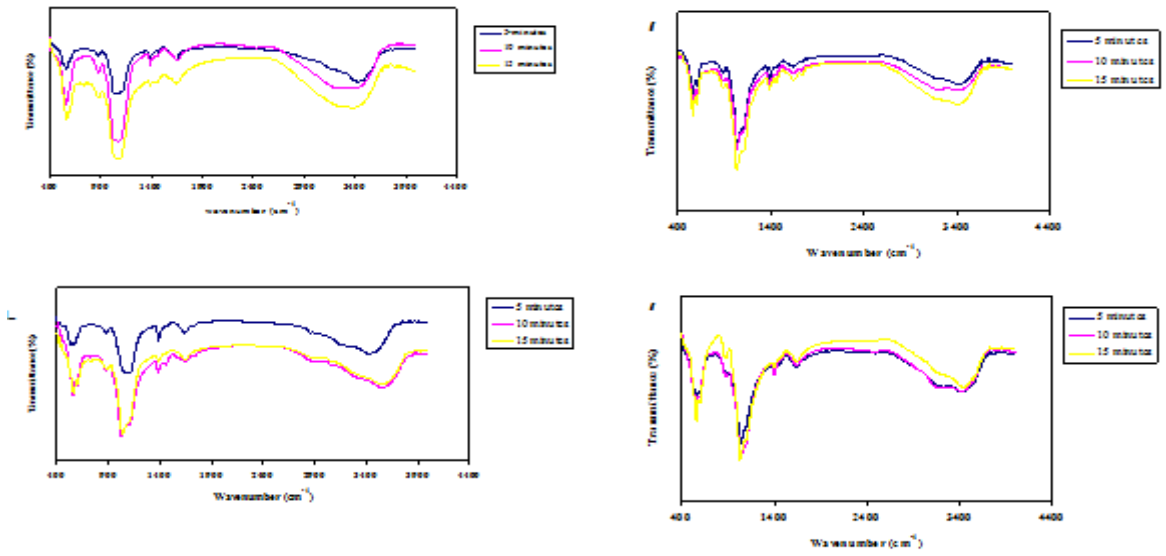

Figure (4) FTIR spectra of HAp formation at different emulsification speed, a)8000 rpm, b)10000 rpm, c)12000 rpm and d)14000 rpm, & constant other parameters.

The size and morphology of HAp nanoparticles produced at different emulsification speed (8000 – 14000 rpm) and 5 minutes constant emulsification time were analyzed by TEM as presented in Figure (5). It can be seen that, all of the HAp synthesized particles are spherical or close to spherical in shape with different sizes. As emulsification rotating speed increases from 8000 rpm to 14000 rpm, the particle diameter size decreases approximately from 38 nm to 7 nm as expected, since it is well established that higher agitation intensity produces smaller internal droplet size which controls the size of the final product.

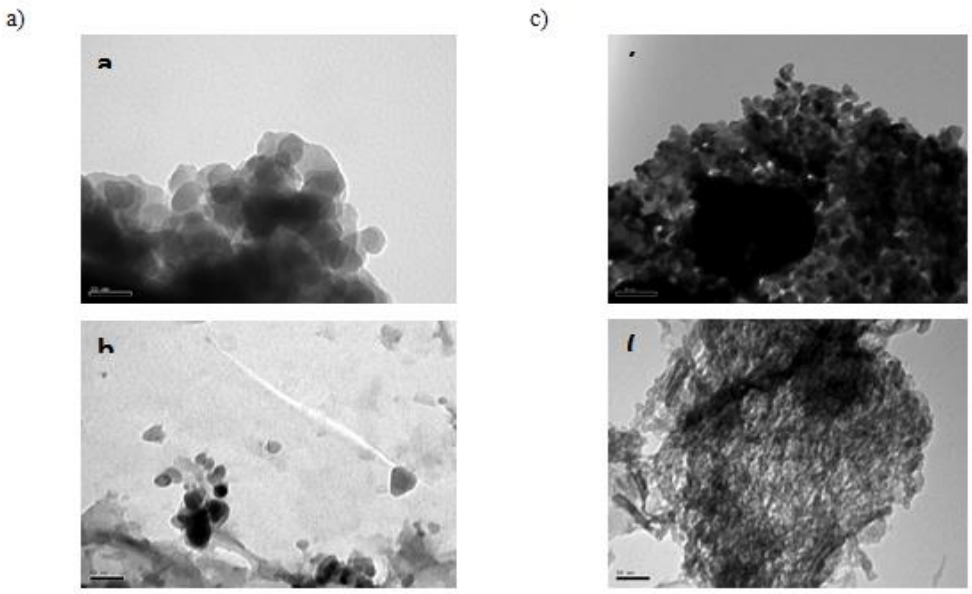

Figure (5) TEM images of HAp nanoparticles prepared at different emulsification speeds a)8000 rpm, (b) 10000 rpm, (c) 12000 rpm and (d)14000 rpm, & other constant parameters.

ISSN: 0975-8585

The XRD pattern of HAp nanoparticles, synthesized at pre-optimized emulsification time and emulsification speed (5 minutes and 14000 rpm respectively) and other constant conditions, is illustrated in Figure (6). The XRD peaks are attributed not only to HAp lattice planes, but also to brushite lattice planes. The major diffraction peaks correspond to the peaks of HAp representing about 95% of the powder product and the minor peak of brushite represents about 5% of the powder; this data confirmed the results obtained from FTIR analyses.

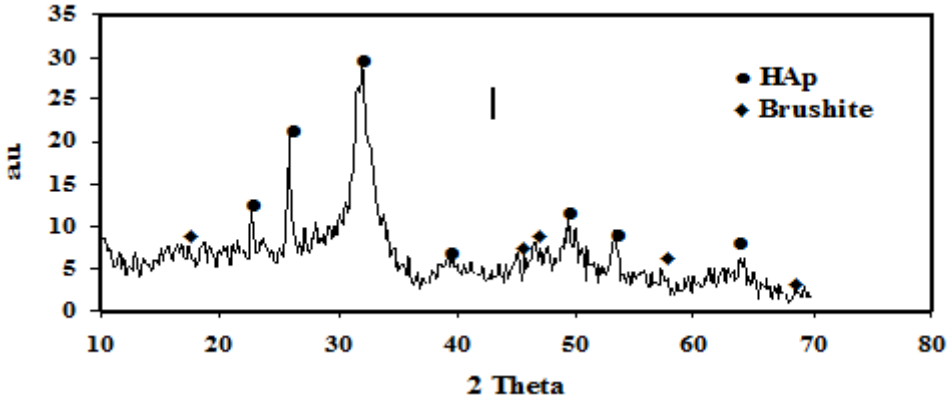

Figure (6) XRD pattern of HAp nanoparticle prepared at 5 minutes emulsification time and 14000 rpm emulsification speed.

Effect of mixing speed

ELM stability

The influence of mixing speed ranging from 200 to 450 rpm on the behavior of the emulsion stability is illustrated in Figure (7), at constant operating conditions: 5min. emulsification time, 14000 rpm emulsification speed, 4% w/v D2EHPA, 4% w/v span 80 and kerosene as organic solvent. It can be observed that, operating at lower mixing speeds (200-250 rpm), the breakage percentage of the emulsion is decreased. With increasing mixing speeds from 250 to 350 rpm, it becomes nearly constant, while further increasing to 450 rpm lead to higher breakage percentage of the emulsion. This is mainly due to that when the external interfacial area is increased by increasing mixing speeds, the ejection of the internal phase is facilitated [21], and that an excessive stirring speed produce coalescence and finally breakdown of globules, making the primary emulsion unstable [22]. Therefore, it is very important to select a suitable mixing speed conditions during the process in order to maintain adequate membrane stability and minimize the emulsion swelling.

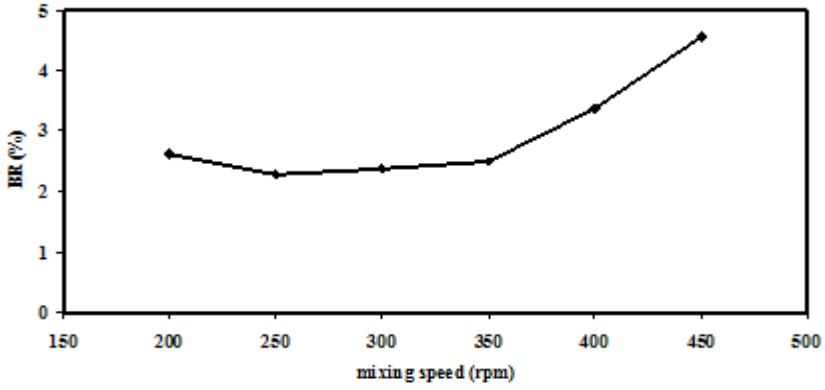

Figure (7) Effect of mixing speed on emulsion stability at 5 min. emulsification time, 14000 rpm emulsification speed, 4% w/v D2EHPA conc., span 80 conc. 4% w/v and kerosene solvent.

ELM efficiency

At similar operating conditions as above, the transfer of calcium ions from external phase to internal phase through the liquid membrane, during the preparation of HAp nanoparticles, is directly proportional with mixing speed from 200 to 350 rpm as shown in Figure (8). This is owing to that when mixing speed is increased, the emulsion globules size decreases accompanied by an increase in the interfacial area available for mass transfer, which consequently leads to the escalation of calcium ions extraction efficiency from 87.65 to 98.65 %. However, there is an upper limit for this effect (350 rpm) where the shear exerted on liquid membrane particle may break the membrane, and thus reduce the efficiency of the whole process. This result is in good agreement with reported work [23-25].

From the above results, it can be concluded that to fulfill the demands of well dispersing in addition of low emulsion breakage, the best suitable mixing speed is selected to be 350 rpm as this value ensure a good stability of the W/O emulsion and enhance the interfacial area available for mass transfer for the subsequent experiments.

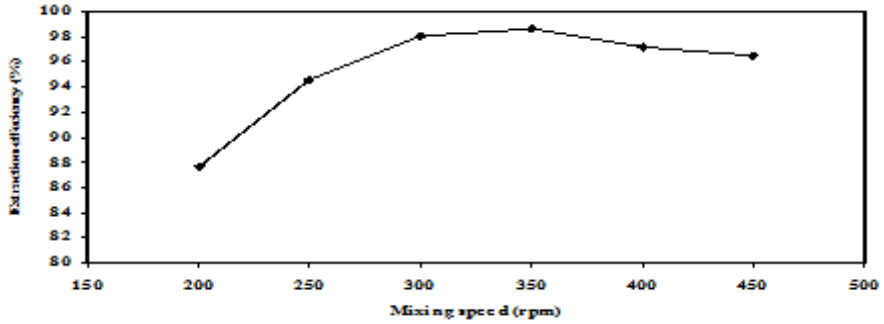

Figure (8) Effect of mixing speed on extraction efficiency of Ca^{+2} at 5 min. emulsification time, 14000 rpm emulsification speed, 4% $_{w/v}$ D2EHPA conc., 4% $_{w/v}$ span 80 conc. and kerosene solvent and organic solvent (kerosene).

Characterization

Figure (9) illustrates the XRD patterns of HAp nanoparticles prepared at different mixing speeds (200 – 450 rpm).

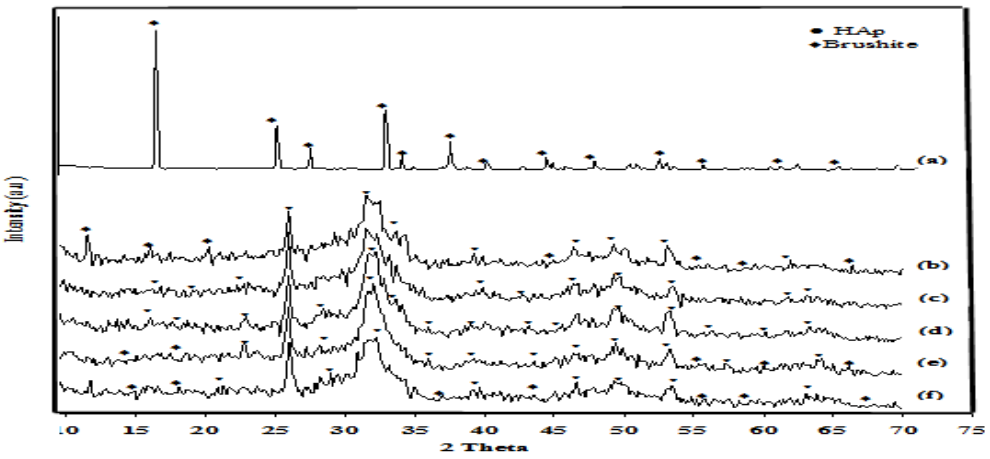

Figure (9) XRD patterns of HAp synthesized at various mixing speeds (a) 200 rpm, (b(c) 300 rpm, (d) 350 rpm, (e) 400 rpm and (f) 450 rpm.

It is noticed that the high intensity diffraction peaks of the product prepared at 200 rpm (Figure 9a) are assigned to mainly brushite phase, no characteristic peaks of other calcium phosphate phases or impurities were detected. The intensity of the diffraction peaks indicates that the sample was well crystallized. While the

ISSN: 0975-8585

broad diffraction peak, appeared in Figure (9b) during increasing the mixing speed to 250 rpm, is corresponding to HAp phase combined with traces of brushite. When mixing speed is extended to 300 rpm, (Figure 9c), all the peaks corresponding to brushite have disappeared and only those belonging to HAp are detectable. Further increasing of mixing speed to 350 rpm, (Figure 9d), results in further increase in the crystallinity of the HAp as evidenced by the further sharpening of the principle diffraction peaks. By increasing the mixing speed from 400 to 450 rpm, the peak of brushite starts to appear again with different amounts. This is probably due to emulsion instability at these speeds, which reduces the transfer of calcium ions from external phase to the internal phase during the preparation of HAp, as was previously observed in Figures (9e & 9f).

TEM images of HAp nanoparticles formed at different mixing speeds (200-450 rpm) are presented in Figure (10). It is found that, the morphology of the sample prepared at 200 rpm (Figure 10a) is mainly elongated plates with length up to130 nm and diameter around 13.3 nm. Increasing mixing speed from 250 to 350 rpm, the sample morphology was transformed to needle-like. The length and diameter of these needles are changed with varying mixing speeds, where the diameter increase is accompanied by a length decrease ranging from 4-7 nm to 5-8 nm and from 40-90 nm to 30-50 nm respectively, as demonstrated in Figures (10b, c and d). Further increasing in mixing speeds (400 - 450) rpm converted the morphology of HAp nanoparticles to spheres with diameter range 7-10 nm. Thus, the results indicate that the mixing speed play an important role in the size and morphology of the product: At the lower mixing speed, the transfer rate of calcium ions is slower and calcium ions, which come to the inner phase, first form a few crystal nuclei of the sample. This nucleus gradually settle on it to form long plates. However, at higher mixing speed, the transfer rate of calcium ions becomes quicker and the numbers of HAp nucleus is formed at a very short time, and the particles generated are smaller and the appearance is spheres. In addition, the change of mixing speeds from low (200 rpm) to high (450 rpm) changes the amount of calcium ions transferred from feed phase to the internal phase and this consequently affects the type of the formed sample such as brushite, HAp or mixture of them.

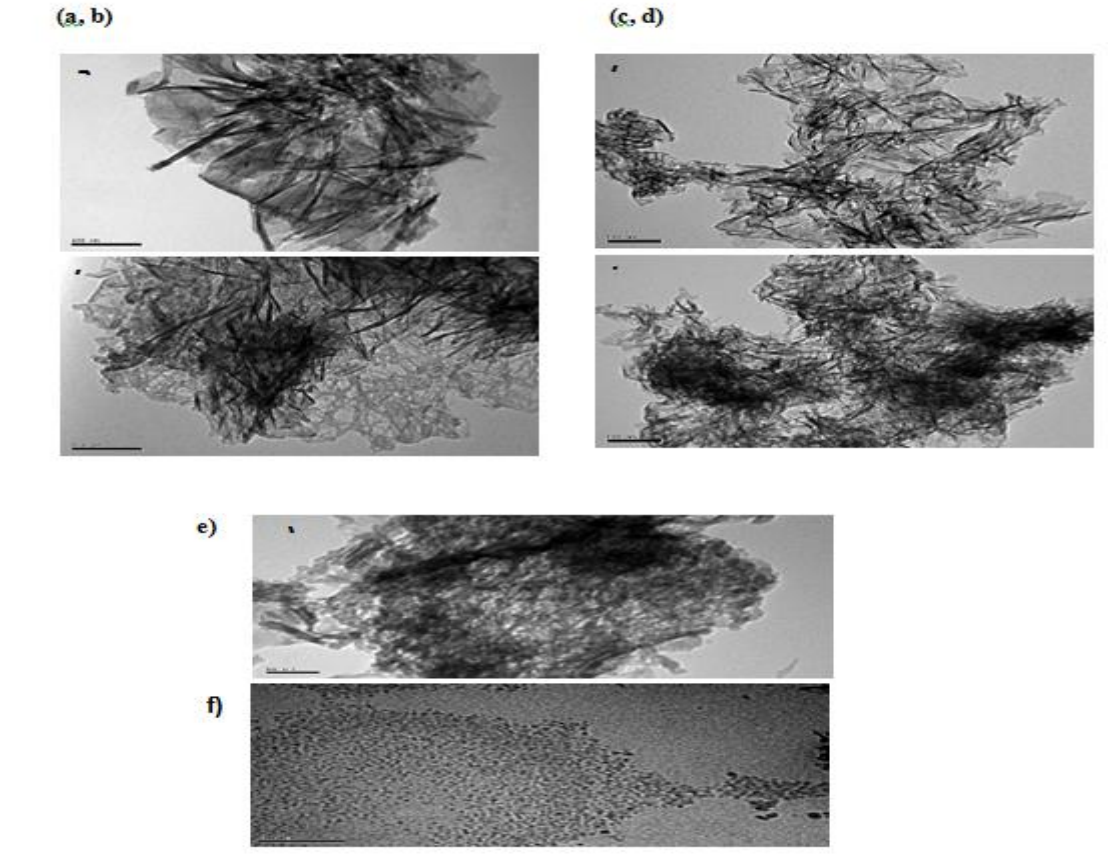

Figure (10) TEM images of Hap nano particles prepared at various mixing speeds (a) 200 rpm, (b) 250rpm, (c) 300 rpm, (d) 350 rpm, (e) 400 rpm and (f) 450 rpm

ISSN: 0975-8585

Effect of type and concentration of carrier

ELM stability

As the solubility of Ca^{2+} ion in organic solvent inhibits its transfer through the ELM, the assistance of a suitable carrier is thus recommended. Hence, this study selected two types of extractants to be investigated: an organo phosphorus and a carboxylic acid, namely D2EHPA and n-caproic acid respectively. The effect of carrier types and concentration (3-9 % $_{w/v}$) on emulsion stability is illustrated in Figure (11). The experimental runs were performed at constant operating conditions: 14000 rpm emulsification rotating speed, 5 min. emulsification time, 350 rpm mixing speed, 4% $_{w/v}$ Span 80 concentration and kerosene solvent.

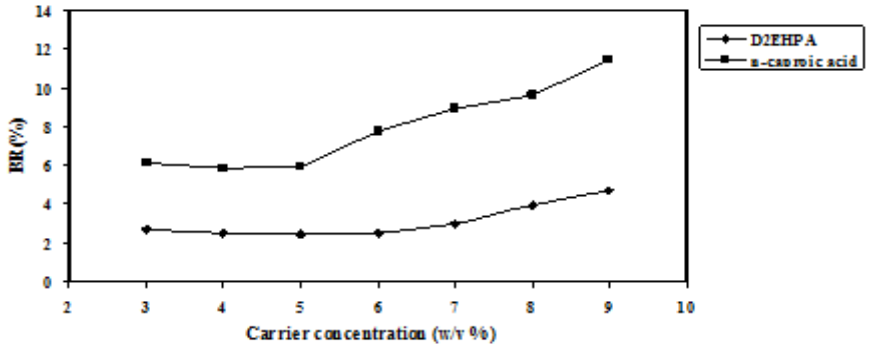

Figure (11) Effect of carriers on ELM stability at emulsification time (5 min.), emulsification speed (14000 rpm), mixing speed (350 rpm),surfactant conc. (5% $_{w/v}$) and organic solvent (kerosene)

It is observed that, increasing the carrier concentration in the membrane phase from 3-5% $_{w/v}$, leads to minor decrease in breakage percentage. This behavior may be caused by increasing the membrane viscosity slightly, which enhances the emulsion stability. At first sight, the use of n-caproic acid has a negative effect on the emulsion stability, as it gives higher breakage rate percent. In case of D2EHPA, elevating its concentration in the membrane (6-9 %$_{w/v}$), decreases the emulsion stability, where the surfactant was decomposed by the presence of D2EHPA due to its catalytic activity on the reaction rate of the surfactant decomposition. Also, it was reported [25] that swelling phenomenon was observed when carrier concentration increased because D2EHPA is an anionic surfactant in nature, the stability of w/o emulsion in its presence would decreases due to water transport from aqueous feed phase.

ELM efficiency

The effect of n-caproic acid and D2EHPA concentrations on transportation of calcium, from external phase to the internal phase through liquid membrane, is demonstrated in Figure (12). As expected from above results, D2EHPA carrier have the best behavior on the removal efficiency of calcium.

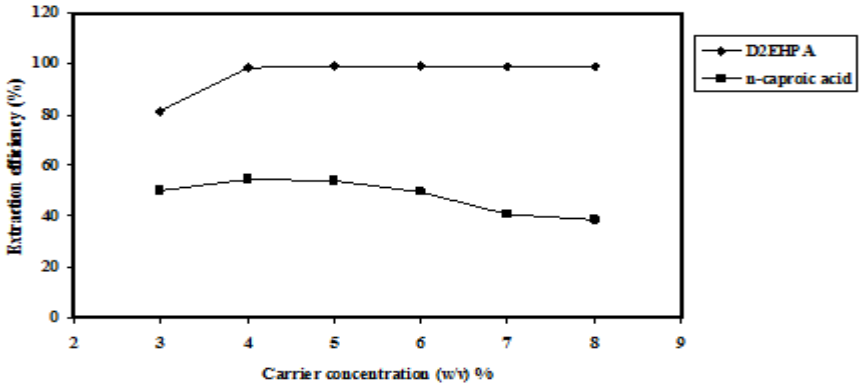

Figure (12) Effect of carriers on removal efficiency of calcium at 5 min. emulsification time, 14000 rpm emulsification speed, 350 rpm mixing speed, 4%$_{w/v}$ span 80 conc. and kerosene

ISSN: 0975-8585

When increasing the concentration of D2EHPA from 3%$_{w/v}$ to 4%$_{w/v}$, the removal efficiency of calcium increased from 81.25% to 98.65 %, compared with n-caproic acid where the removal efficiency increased only from 49.95% to 54.55%. While further increasing in carrier concentration does not remarkably affect the extraction performance. Since the carrier is the most expensive agent among the other components of the liquid membrane system, its lower concentration is always preferred (4% $_{w/v}$).

Characterization

The FTIR spectra of HAp nanoparticles, prepared at different D2EHPA carrier concentrations (3% $_{w/v}$ - 8% $_{w/v}$), is demonstrated in Figure (13). The results indicate that most of the spectra are corresponding to the bands of Hap. As D2EHPA concentration increases up to 5% $_{w/v,}$ the absorption intensity of OH stretching vibration band at 3572 and 633 cm^{-1} increased, which are the most bands attributed to HAp formation.

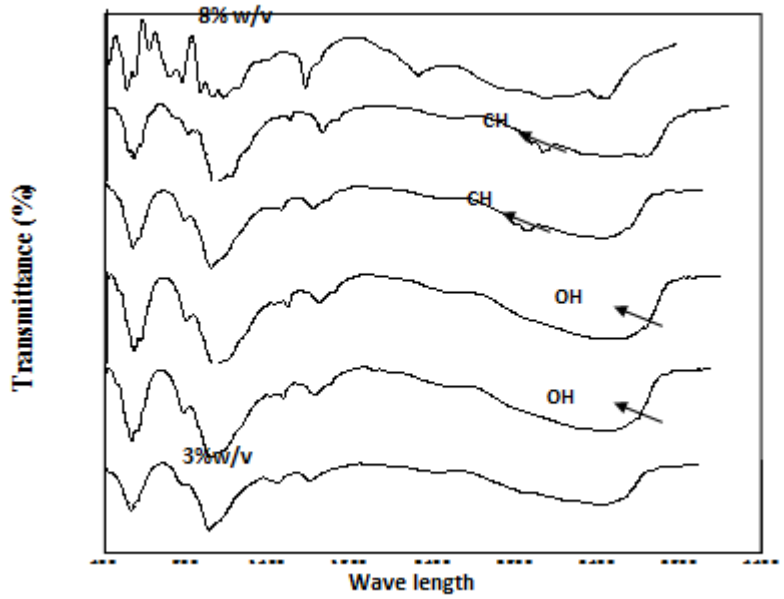

Figure(13) FTIR spectra of HAp formation at different carrier concentrations (D2EHPA)

Further increasing of D2EHPA concentration is joined to the appearance of CH stretching vibration band. The presence of such band may be due to surfactant decomposition, resulted from the catalytic activity of the carrier on the reaction rate of the surfactant as mentioned earlier above.

The TEM image of HAp nanoparticles synthesized at 4%$_{w/v}$ D2EHPA concentration is presented in Figure (14). In presence of D2EHPA, the HAp nanoparticles showed needle-like morphology with average length in the range of 30-50 nm and diameter of 5-8 nm.

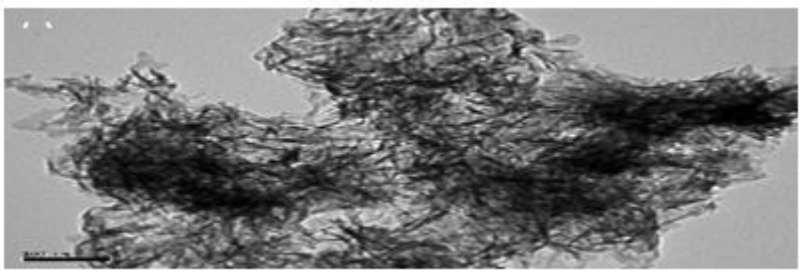

Figure (14) TEM image of HAp nanoparticles prepared at 4%$_{w/v}$ D2EHPA carrier concentration.

ISSN: 0975-8585

Effect of type and concentration of surfactant

ELM stability

The lipophilic nonionic surfactants of the sorbitan fatty acid ester types, namely Span 20 (sorbitanmonolaurate), Span 80 (sorbitanmonooleate) and Span 83 (sorbitansesquioleate) were selected to investigate their effects at different concentrations (3%$_{w/v}$-9%$_{w/v}$) on the emulsion stability. The experiments were conducted at pre-optimized conditions, i.e.,14000 rpm emulsification rotating speed, 5 min. emulsification time, 350 rpm mixing speed, and 4%$_{w/v}$ D2EHPA carrier concentration, with kerosene as organic solvent. The influence of surfactants type and concentration on emulsion stability is illustrated in Figure (15).

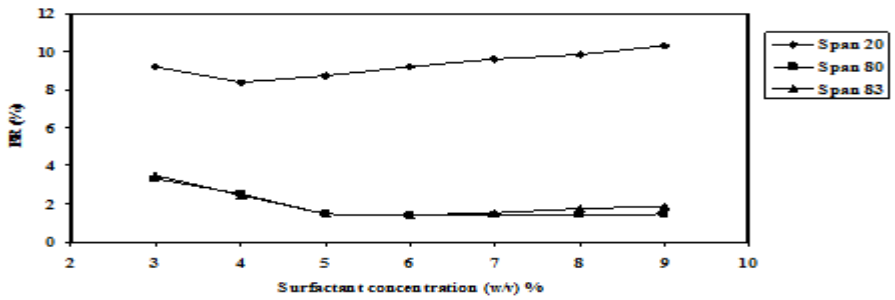

Figure (15) Effect of surfactants on ELM stability at 5 min. emulsification time, 14000 rpm emulsification speed, 350 rpm mixing speed, 4%$_{w/v}$ D2EHPA conc. and kerosene

As observed, Span 20 gives the lowest stable emulsion than other surfactants at all concentrations; this may be attributed to the relatively higher polarity of this surfactant than the other surfactants - owing to its shorter fatty acid chain length - resulting in aqueous phase solubilization where this apparently hinders interfacial molecular interactions and consequent multilayer buildup [26]. While, two surfactants (Spans 80 & 83) are nearly having the same behavior in the emulsion stability: as surfactant concentration increases up to 5%$_{w/v}$, the emulsion stability increases, then becomes nearly constant with minor lessening in membrane stability in case of Span 83 over 7%$_{w/v}$ concentration. This behavior may be owing to the higher stability transmission initially to the membrane by surfactant concentration, caused by the increased number of surfactant monolayers absorbed onto the micro-droplet interface. Further increase, in these layers, leads to a droplet stability increase up to a preventive value where the droplet surface became saturated with surfactant monolayer. Beyond this value, higher surfactant concentration ceases to further increase in membrane stability; on the contrast, its action results in membrane decay [27].

ELM efficiency

The effect of surfactant on the behavior of calcium extraction for the preparation of HAp nanoparticles is illustrated in Figure (16).

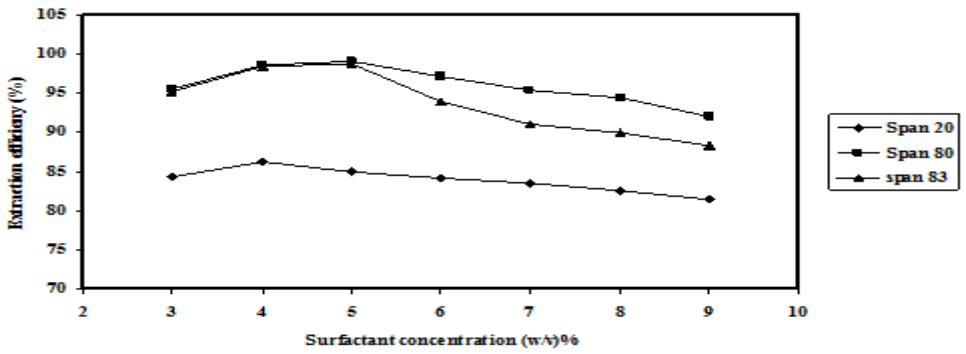

Figure (16) Effect of surfactants on extraction efficiency of calcium at 5 min. emulsification time, 14000 rpm emulsification speed, 350 rpm mixing speed, 4% w/v D2EHPA conc. and kerosene.

As expected, the use of Span 20 results in greater declination in the extraction efficiency due to the breakup of membrane emulsion. While, increasing Span 80 and Span 83 concentrations from 3%$_{w/v}$ to 5%$_{w/v}$ increased Ca^{+2} ions transport from 95% to 99%. Because, in addition to their capabilities of a higher membrane stability, increasing concentration results in higher contact area between the donor and receiving phases and consequently increasing the removal efficiency of calcium. However, excessive amounts of surfactant in membrane phase increase its viscosity, which resists the diffusion of calcium ions through the membrane, and consequently reduced the mass transfer of calcium ions. The higher efficiency decrease, observed with the use of Span 83, is probably caused by the differences in surfactants molecular weights (Span 80 MW= 428 g/mole and Span 83 MW = 560 g/mole) which affect the membrane phase viscosity.

Characterization

The TEM images of HAp nanoparticles produced at different Spans (80 and 83) at 5%$_{w/v}$ concentration are shown in Figure (17).

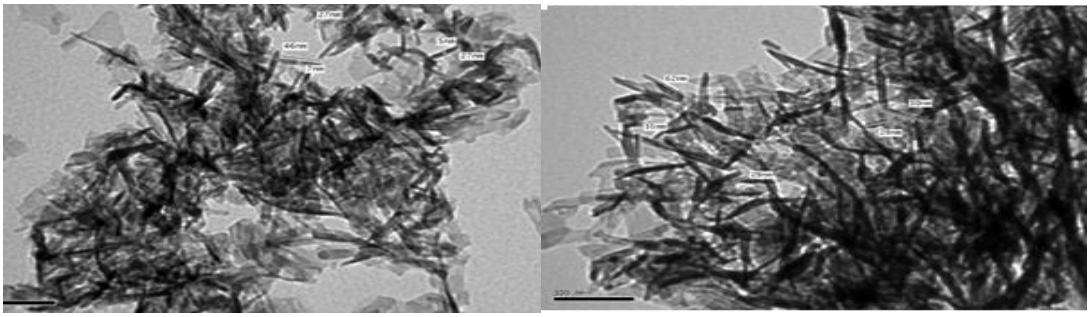

(a) (b)

(a) Figure (17) TEM images of HAp nanoparticles prepared at different surfactants: (a) Span 80 and (b) Span 83

The images reveal that, the morphology of the prepared Hap nanoparticles in presence of Span 80 is needle-like shape with, diameter range 3-7 nm and length 27-46 nm as depicted in Figure (17a). While liquid membrane containing Span 83 as surfactant yields HAp nanoparticles in rode form, with larger diameter and length ranges [(4-10 nm)& (29-100 nm) respectively] as shown in Figure (17b). The differences in the morphology of the product prepared by using various surfactants may be due to the differences in the properties of the two surfactants, especially the hydrophile-lyophile balance (HLB), which has values of 4.3 and 3.7 for Span 80 and Span 83 respectively.

Effect of organic solvent type

ELM stability

Figure (18) illustrates the emulsion stability using different types of organic solvents, namely, kerosene, iso-octane, heptane, hexane and toluene, at best conditions previously established: 14000 rpm emulsification rotating speed, 5 min emulsification time, 350 rpm mixing speed, 4% $_{w/v}$ D2EHPA concentration and 5% $_{w/v}$ Span 80 concentration.

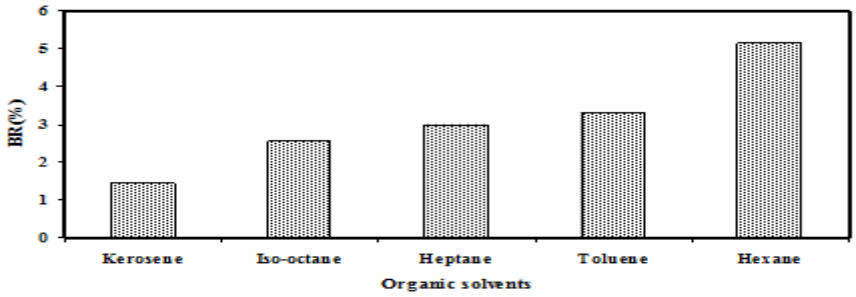

Figure (18) Effect of organic solvents on ELM stability at 5 min. emulsification time, 14000 rpm emulsification speed, 350 rpm mixing speed, 4% $_{w/v}$ D2EHPA conc. and 5% $_{w/v}$ Span 80 conc.

As noticed, the membrane stability increased in the following order: kerosene >iso-octane > heptane > toluene > hexane. These results indicate that aliphatic diluents are generally preferred than aromatic, due to their low water solubility and thus, produce better emulsion stability. Furthermore, emulsion comprising aromatic diluents lean towards breaking-down under shearing condition, owing to water permeation from the external phase to the internal phase through the thin oil layer. Moreover, kerosene provides better performance that is probably due to solvation effect in the membrane solution, since the requirement is for a solvent that allows a reasonable concentration of the extractant at the interface whilst dissolving sufficient extracted complex. In addition, kerosene has higher viscosity compared to other solvents, which produces good stability, as lower viscosity may cause poor transport rate and thus, has a negative effect on the emulsion stability [30]. On the other hand, the higher number of carbon atoms in kerosene means a higher hydrophobicity, which results in less transport of water across liquid membrane than when using other solvents as previously reported [28]. Hence, from the obvious results, kerosene is selected as best organic solvent in liquid membrane for the preparation of HAp nanoparticles.

Characterization

The FTIR spectrum of HAp nanoparticles prepared in presence of the kerosene solvent is demonstrated in Figure (19).

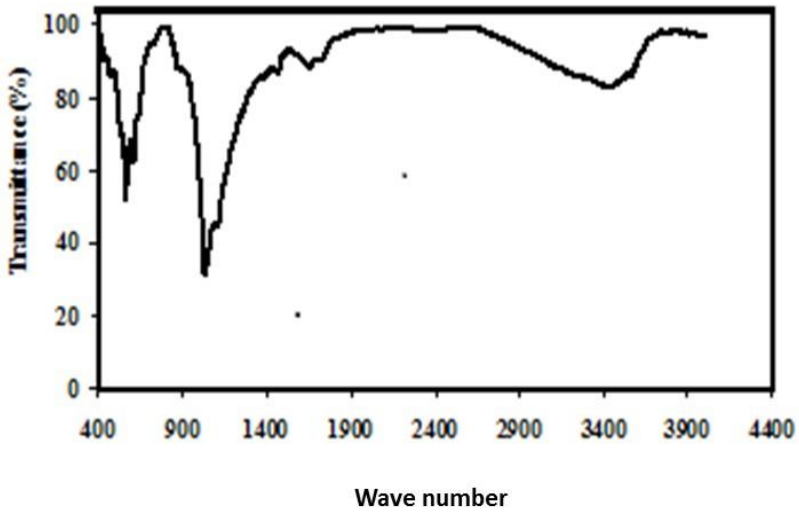

Figure (19) FTIR spectra of HAp prepared with kerosene solvent.

The result indicates that most of the peaks are attributed to two vibration modes: (1) the stretching mode of PO_4^{3-} occurring at 565, 603, 965 and 1031 cm^{-1}; and (2) the stretching mode of OH^- occurring at about 3572 cm^{-1}. The latter is shown as a tiny shoulder of the H-O-H peak between 3400 and 3450 cm^{-1} owing to the stretching mode of H-bonded OH^- or water [29]. The small bands appearing at wave number values of 1402-1462 and 879 cm^{-1} reveal the presence of carbonate ions in the resultant HAp due to the interaction between HAp and ambient CO_2 in the processing [30]. Further, the results showed that the absorption band derived from PO_4^{3-}reveals that kerosene solvent produced HAp nanoparticles with high crystallinity.

The TEM images of the synthesized HAp nanoparticles by ELM system comprising different organic solvents are presented in Figure (20).

ISSN: 0975-8585

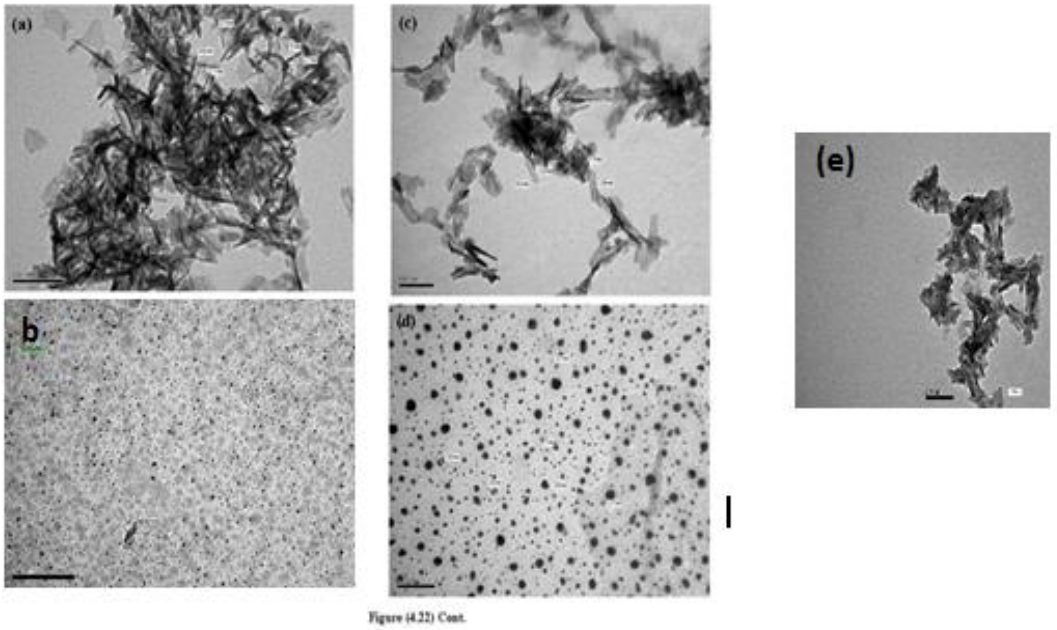

Figure (20) TEM images of HAp prepared at different organic solvents: (a) kerosene, (b) iso-octane, (c)heptane, (d)toluene and (e) hexane.

On investigating the TEM results, it has been observed that the type of organic solvent plays a significant role in the size and morphology of the prepared HAp nanoparticles. It demonstrates that HAp prepared by using kerosene display a uniform nano-needles with diameter ranging 3nm to7nm, and 27nm to 46nm in length, as presented in Figure (20a).

CONCLUSIONS

The present work aimed, mainly, at preparing hydroxyapatite compound in nano form by means of an innovative technique, namely, emulsion liquid membrane. The important parameters, having the greatest influence on the stability of the emulsified liquid membrane and consequently on the HAp nanoparticle synthesis were determined. Emulsification rotating speed proved great impact on emulsion stability, calcium extraction efficiency, size and crystallinity of the prepared Hap. The change of mixing speeds affect the type of the formed particles, such as brushite, HAP or mixture of them, and this consequently affect the morphology and size of the final product, i.e., plates, needles and spheres, which subsequently govern the product application domains. Further, the solvent type has significant effect on membrane stability and product morphology. Finally, the preparation of needle-like HAp nano particles with diameter in the range 3-7 nm and 27-46 nm in length is achieved at :14000 rpm rotating speed, 5min. emulsification time, 350 rpm mixing speed, 4%$_{w/v}$ D2EHPA carrier concentration, 5%$_{w/v}$ Span 80 surfactant concentration and kerosene organic solvent.

REFERENCES

[1] Zhang, H., Zhou, K., Li, Z., Huang, S. "Plate-like hydroxyapatite nanoparticles synthesized by the hydrothermal method", Journal of Physics and Chemistry of Solids 70 (2009) 243–248

[2] Kumar, R.A., Kalainathan, S. "Sol–gel synthesis of nanostructured hydroxyapatite powder in presence of polyethylene glycol" Physica B 405 (2010) 2799–2802

[3] Tabrizi, N.B., Honarmandi, P., Kahrizsangi, E. R. "Synthesis of nanosize single-crystal hydroxyapatite via mechanochemical method" Materials Letters 63 (2009) 543–546.

[4] Li, C., Wang, P., Gong, H., Jiang, X., Wang, H., Li, "Effects of synthesis conditions on the morphology of hydroxyapatite nanoparticles produced by wet chemical process." Powder Technology, 203 (2010) 315-321.

[5] G.N.ManikandanK.Bogeshwaran*, P.Jamuna, S.Sandhya "A Review on Emulsion liquid Membranes on heavy metal separation, International Journal of ChemTech Research, Vol.6, No.9, pp 4328-4332, September (2014)

[6] Yuzhang Zhu, Dong Wang, Lei Jiangand Jian Jin˝ Recent progress in developing advanced membranes for emulsified oil/water separation", Asia Materials (2014) 6.May 2014

[7] A.T.Kassem, *N.El-said, and H, F.Aly "Application of emulsion liquid membranes for removal of Cd ,Co,Ni and Pb from Ismailia Canal, red sea, El Manzala lake, tape waters.Journal of Applied Chemistry Volume 6, Issue 4 (Nov. – Dec. 2013), PP 45-52

[8] Jarudilokkul, S., Tanthapanichakoon, W. and Boonamnuayvittaya, V. "Synthesis of hydroxyapatite nanoparticles using an emulsion liquid membrane system." Colloids Surf. A, 296 (2007)149-53.

[9] Rania. M.Sabry" Heavy metal separation from industrial wastewater by using Emulsified liquid membrane in Egypt and Tunisia, theses MSc (2006).

[10] Valenzuela, F., Cabrera, J., Basualto, C. and Hagar, J. S. (2005). Kinetics of copper removal from acidic mine drainage by a liquid emulsion membrane. Miner. Eng., 18, 1224-32.

[11] Chakraborty, M., Bhattacharya, C., Datta, S. "Study of the stability of w/o/w-type emulsion during the extraction of nickel (II) via emulsion liquid membrane." Sep. Sci. Technol., 39 (2004) 1-17.

[12] Rania. M.Sabry" Heavy metal separation from industrial wastewater by using Emulsified liquid membrane in Egypt and Tunisia, theses MSc (2006).

[13] Rania Sabry, Azza Hafez, MaalyKhedre, Adel Hassanine, Removal of lead by emulsion liquid membrane Part-1, 2006

[14] Hirai,ª T., Hodono, M., Komasawa, I., " The Preparation of Spherical Calcium Phosphate Fine Particles Using an Emulsion Liquid Membrane System" Langmuir, 16 (2000), 955 -960.

[15] RaniaSabry "Preparation of Hydroxyapatite Nanoparticles by using Emulsified liquid membrane, pHD 2012

[16] Kralj, D., Brecevic, L., " Precipitation of some slightly soluble salts using emulsion liquid membrane ", Croatica Chemical Acta 71 (4) (1998),1049-1060.

[17] Bourenane, S. Samar, M.E.H. Abbaci, A. "Extraction of cobalt and lead from wastewater using a liquid surfactant membrane emulsion." ActaChem.Solv. 50 (2003) 663 – 675.

[18] Varma, H.K., Babu, S.S. "Synthesis of calcium phosphate bioceramic by citrate gel pyrolsis method." Ceram. Int. 31, (2005), 109-114.

[19] Singh, S., Bhardwaj, P., Singha, V., Aggarwal, S., Mandal, U. K. "Synthesis of nanocrystalline calcium phosphate in microemulsion - effect of nature of surfactants." Journal of Colloid and Interface Science 319 (2008) 322–329.

[20] Bourenane, S. Samar, M.E.H. Abbaci, A. "Extraction of cobalt and lead from wastewater using a liquid surfactant membrane emulsion." ActaChem.Solv. 50 (2003) 663 – 675.

[21] Valenzuela, F. Fonseca, C. Basualto, C. Correa, O. Tapia, C. Spag, J. "Removal of copper ions from a waste mine water by a liquid emulsion membrane method", mineral engineering 18 (2005) 33 – 40.

[22] Kumbasar, R.A. Tutkum, O. "Separation and concentration of gallium from acidic leach solution containing various metal ions by emulsion type of liquid membranes using topo as mobile carrier", Hydrometallurgy 75 (2004) III – 121.

[23] Jr, C.P.R., Costa, A.O.S., Lopes, I.P.B., Campos, F.F., Ferreira, A.A. and Salum, A. "Cobalt extraction and cobalt-nickel separation from a simulated industrial leaching liquor by liquid surfactant membranes using cyanex 302 as carrier", J. Membr. Sci. 241 (2004) 45-54.

[24] Juang, R.S., Lin, K.H., "Ultrasound-assisted production of W/O emulsions in liquid surfactant membrane process." Colloids Surf. A: Physicochem. Eng. Asp. 238 (2004) 43–49.

[25] Opawale, O.F., Burgess, J.D. "Influence of interfacial properties of lipophilic surfactants on water-in-oil emulsion stability." Journal of Colloid and Interface Science, 197 (1998) 142-150. [27] Pal, P., Dutta, S., Bhattacharya, P. "Studies on the modeling and simulation of a sequential bienzymatic reaction system immobilized in emulsion liquid membrane. Biochem.Eng. J., 5 (2000) 89-100.

[26] Kulkarni, P.S. Mukhopadhyay, S. Bellary, M.P. Ghosh, S.K. "Studies on membrane stability and recovery of uranium (VI) from aqueous solutions using a liquid emulsion membrane process", Hydrometallurgy 64 (2002) 49 – 58.

[27] Kumar, R., Prakash, K.H., Cheang, P., Khor, K. A., Langmuir 20 (2004) 5196.

[28] Cho, J. S., Ko, Y. N. Koo, H. Y., Lee, M. J., and Kang, Y. C. "Effects of solvent on the properties of nano-sized hydroxyapatite powders directly prepared by high temperature flame spray pyrolysis."Journal of Ceramic Processing Research. 10 (5) (2009) 628-632.